FeedNetBack-D08.02- Tools for underwater fleet communication

Jan Opderbecke, Alain Kibangou

GRANT AGREEMENT N°223866

Deliverable	D08.02
Nature	Report
Dissemination	Public

D08.02 – Tools for Underwater Fleet Communication

Report Preparation Date	03/08/2010 Project month: 24
Authors	Jan Opderbecke, P06 – IFREMER Alain Kibangou, P01 – INRIA
Report Version	*V1*
Doc ID Code	DOP/DCM/SM/PRAO/10-307
Contract Start Date :	01/09/2008
Duration :	36 months
Project Coordinator :	Carlos CANUDAS DE WIT, INRIA, France

Theme 3:

Information and Communication Technologies

Table of Contents

1. Executive Summary 4
2. Introduction 4
3. Acoustic multi channel communication 4
4. Acoustic data transmission sea trials 6
5. Modeling of propagation performances 8
Estimation of range in function of sound speed profiling 9
Estimation of range in function of receiver noise level 11
6. Conclusions for AUV fleet control and simulation 13
7. OFDM Receiver for underwater acoustic communications 14

1. Executive Summary

The present document presents work on acoustic vehicle communications networking and potential advances in the field of underwater data transmission in the scope of the FeedNetBack case study (b), work package 8 ‘underwater operation with coordinating vehicle fleet’, and gives practical background on the constraints of signal transmission in the underwater environment.

Second deliverable of WP8, the document is directly continued from deliverable D8.01 ‘case study scenario’ with a focus on scientific and technological background of the underwater communication.

The document’s aim is to provide the projects control approaches with a high level of technical background.

2. Introduction

This document develops a synthesis of the work accomplished in the FeedNetBack project in the area of tools for data transmission between underwater vehicles in a fleet formation.

The global case study scenario has been presented in document D8.01. In paragraph 2 we will resume elements of this underwater fleet case study which are relevant for this document.

A first state-of-the-art networking concept has also been presented in D8.01. Studies of potential improvements of such network architectures are discussed in paragraph 3.

Improved data transmission techniques within commercially available acoustic modems have been evaluated at sea, completing the comparative results from D8.01. The results are presented in paragraph 4.

In the field of underwater signal transmission [1], [2], work has been accomplished in order to understand and better exploit physics of underwater acoustics; specific modeling of sound propagation as to predict propagation performances of acoustic devices in sea conditions is one topic of this work, information theory and Doppler resistant signal coding are complementary approaches.

3. Acoustic multi channel communication

Commercial acoustic data links exist, to our knowledge, exclusively in single channel simplex transfer mode. It is commonly admitted that duplex communication is not realistic on a spatially and frequency limited space on a small underwater vehicle, the reception chain saturation by the high sound pressure level during emission. We will consider in the following that only simplex techniques can be employed, meaning that a transmitting acoustic modem cannot simultaneously receive data.

State-of-the art channel separation techniques like those presented in paragraph 8 do however encourage multi-channel reception. We will in this paragraph analyze in what way hypothetic data

links in simplex mode but multi-channel reception would improve the rate of information exchange in a network of underwater vehicles.

In the following diagrams, we look at the amount of data sets exchanged between N vehicles during N communication cycles.

The vehicles are named V1 through VN, the cycles are C1 to CN. The green color shades represent transmission, the yellow fields represent reception with the number of received data sets being indicated in the grid cell. Case A shows the scenario where only one vehicle emits at one cycle, scenario B shows 2 emitting vehicles, and so forth… Finally the number of received vehicle-data-sets is summed in the horizontal line below each diagram, and the total number is summed up to the right in the red cell.

In a first case we consider **3 vehicles** (figure 1). Two non trivial scenarios A and B exist, with respectively one or two vehicles transmitting their data packets. In both cases 6 data sets are received amongst the fleet, the multi-channel scenario B has not provided an increase in the exchange.

The **4-vehicle**-case in figure 2 shows a total exchange of 12 data sets for one and three transmission channels, and 16 data sets when two simultaneous channels are used. We observe thus a 25% increase.

In a fleet of **5 vehicles**, two and three channel transmissions yield a maximum of 30 exchanged packets, with a 50% increase compared with single channel transmission.

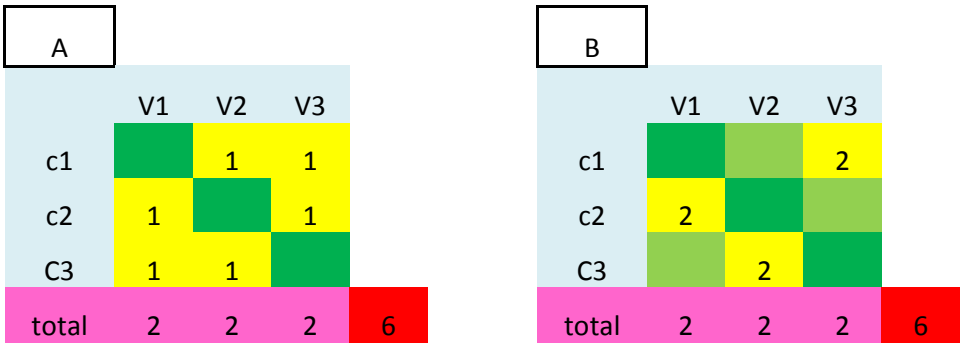

figure 1 : data exchange scenarios for fleet of 3 vehicles

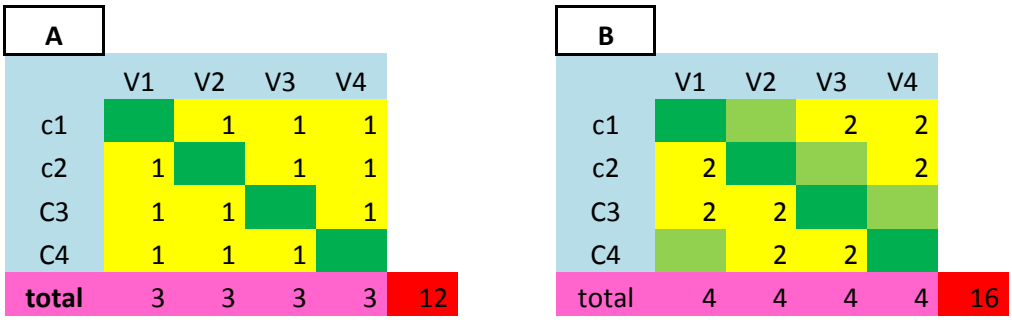

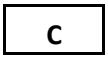

	V1	V2	V3	V4	
c1				3	
c2	3				
C3		3			
C4			3		
total	3	3	3	3	12

figure 2 : data exchange scenarios for fleet of 4 vehicles

A

	V1	V2	V3	V4	V5	
c1		1	1	1	1	
c2	1		1	1	1	
C3	1	1		1	1	
C4	1	1	1		1	
C5	1	1	1	1		
total	4	4	4	4	4	20

B

	V1	V2	V3	V4	V5	
c1			2	2	2	
c2	2			2	2	
C3	2	2			2	
C4	2	2	2			
C5		2	2	2		
total	6	6	6	6	6	30

C

	V1	V2	V3	V4	V5	
c1				3	3	
c2	3				3	
C3	3	3				
C4		3	3			
C5			3	3		
total	6	6	6	6	6	30

D

	V1	V2	V3	V4	V5	
c1					4	
c2	4					
C3		4				
C4			4			
C5				4		
total	4	4	4	4	4	20

figure 3 : data exchange scenarios for fleet of 5 vehicles

As conclusion, we may state that a moderate gain in the information exchange can be achieved with multi – channel technology. As we will see in paragraph 7, a comparable gain can be obtained by higher robustness to multi-pathing and inter channel crossing, by optimized coding techniques within each channel and so reducing guard times included in each transmission slot.

4. Acoustic data transmission sea trials

High data rates of up to10 kbit/s have been evaluated with a commercial acoustic link by sea trials in March 2010 with Ifremer's asterX AUV on the *R/V L'Europe*.

In previous work we have experienced low data rates at 100bit/s [D8.1] to be reliable. Links with higher data rate were appropriate for low noise environments, especially in vertical geometric conditions suitable for mooring-to-surface communications. Data transfer between several underwater

vehicles and between underwater vehicles and surface crafts does not correspond to those criteria, thus opposing transfer through higher rates.

The trials were conducted during the campaign “ESSAUV” on board Ifremer’s RV L’Europe, with the asterX AUV. The tested equipments were Sercel MATS 300 acoustic modems. The following table shows the rate of successful data transfer between the vessel born modem and the AUV modem, in a cycle with down loading and uploading packet streams. The noise level is measured being appr. 74dbµPa√Hz.

Data rate Bit/s	Cycles	Completed	Reliability [%]	Vehicle depth [m]	Slant range in test [m]	Est. max range [m]	
100	n.c.	n.c.	95	0- 2000	200 – 3000	3000	
1000	20	14	70	800	1000	1800	
2000	20	13	65	800	1000	1600	
4000	20	16	80	800	1000	1500	
6000	20	18	90	800	1000	1400	
10000	20	16	80	800	1000	1400	

table 1 : sea-trial evaluation of bit rates from 100bit/s up to 10kbit/s

The results prove that significant improvement has been accomplished on vehicle-to-vehicle and vehicle-to-surface communications. Exchange of more complex data sets concerning vehicle state, possibly payload samples, becomes realistic. The communication is today still based on simplex mode, which leads, together with the transmission delays, to rather simple architectures like TDMA.

The practical evaluation of the maximum transmission range is completed by computation of the theoretical values. The blue series corresponds to a hypothetic low noise vehicle (64dbµPa√Hz), the red one corresponds to the actual noise level of the Ifremer AUVs (74dbµPa√Hz).

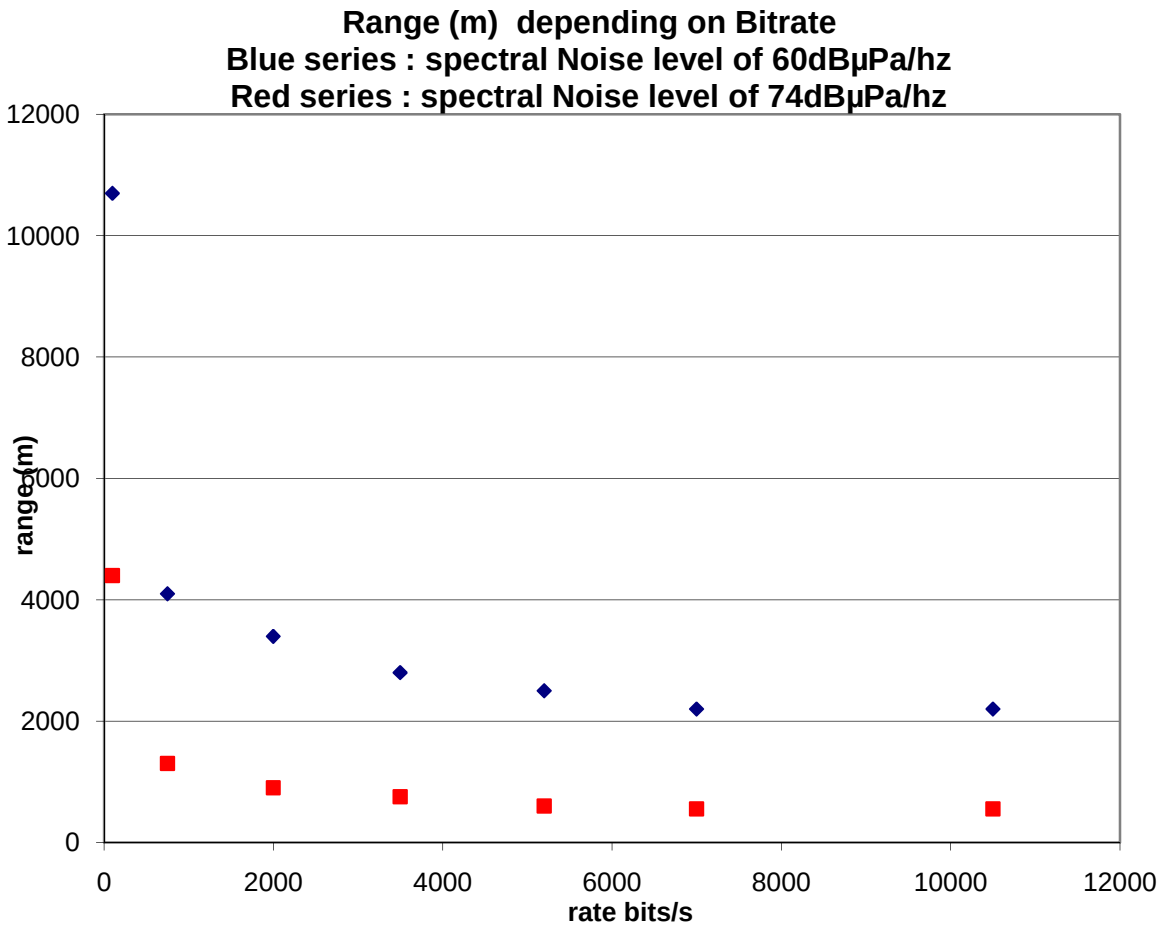

figure 4: transmission range in function of data bit rate

5. Modeling of propagation performances

We are studying the performances of acoustic data transmission in vehicle-to-vehicle conditions. In fact, sound speed variability in water layers, multi-pathing caused by ground or sea-surface reflexion of sound waves, have a significant influence on the transmission quality and range. These performances depend widely on the actual geometry of the transmission problem as given by the vehicle positions. The simulation of the underwater communication benefits from this topic by increasingly realistic modeling.

Issued by cooperation between IFREMER and the French company CHRISAR, a computation model of acoustic signal propagation in function of environmental and technical parameters has been developed and calibrated by sea trials. As a result a software tool with vocation of operational pre-dive evaluation of the performances acoustic transmission systems.

The modeling software allows predicting the margin of the signal-to-noise ratio (SNR) of the acoustic power at the receiver, i.e. the SNR exceeding the minimum level necessary for reception and decoding. The SNR margin can be used to calculate the transmission range at a given threshold of bit error rate, at which a regular the transmission is considered realistic. From the SNR margin we can also determine the bit-error-rate at a given range. The parameters entering the estimation are:

- the acoustic central frequency ;

- the emission power level ;
- the bandwidth of the signal ;

On the technical side the relevant parameters are

- type of seafloor ;
- sea surface state ;
- sound velocity profile;
- acoustic noise power level at receiver;

The software shows as a result in a 2 dimension graph, color-coded reception level as the SNR margin. The maximum range is considered equaling the limit of 0db in the received signal strength. The following paragraphs will consider this latter case of maximum operation range estimation using the 0db signal excess limit. In the graphs, this is the transition from green to yellow colored areas.

The objective of this study is to provide scientific and technological soundness to the concepts of communicating underwater vehicle fleets. The typical technical and operational constraints of underwater system technology are taken into account and add to the realism of the case study.

Estimation of range in function of sound speed profiling

The following computation shows the influence of the sound velocity profile on the transmission conditions and performances. We present computations for a) summer and b) winter, in the case of 100bit/s data rate.

We consider an acoustic modem working at 10kHz at a transmission power of 185dBµPa√Hz, with a bandwidth of 3kHz, a reception band of 240Hz, a detection limit SNR of 10db, and a bit rate of 100bit/s. The environment is characterized by calm surface conditions (no significant wind & wave), a vehicle noise of 64dbµPa√Hz, uniform and flat ‘muddy’ sea floor.

Mediterrenean Sea (Toulon - France) - Summer conditions

In summer periods, the warmth of the surface water layer decreases rapidly in the first meters of depth, and sound velocity decreases with it. After reaching a minimum value at some tens of meters of depth, the sound velocity increases naturally with pressure.

This sound velocity profile causes shadow zones in which a signal will not be received, even if otherwise it would be sufficiently close to be properly received, this phenomenon is typically described by ‘diving rays of sound’.

The plot hereunder represents transmission performance between two vehicles, one diving at 10m depth, the second on diving at

a) the same depth (10m),
b) 100m depth,
c) 300m depth.

In case a) the max range is about 1km, in case b) it is roughly 2km and in c) it is 3km. For depth differences greater than 300m between both vehicles the maximum range will then progressively decrease.

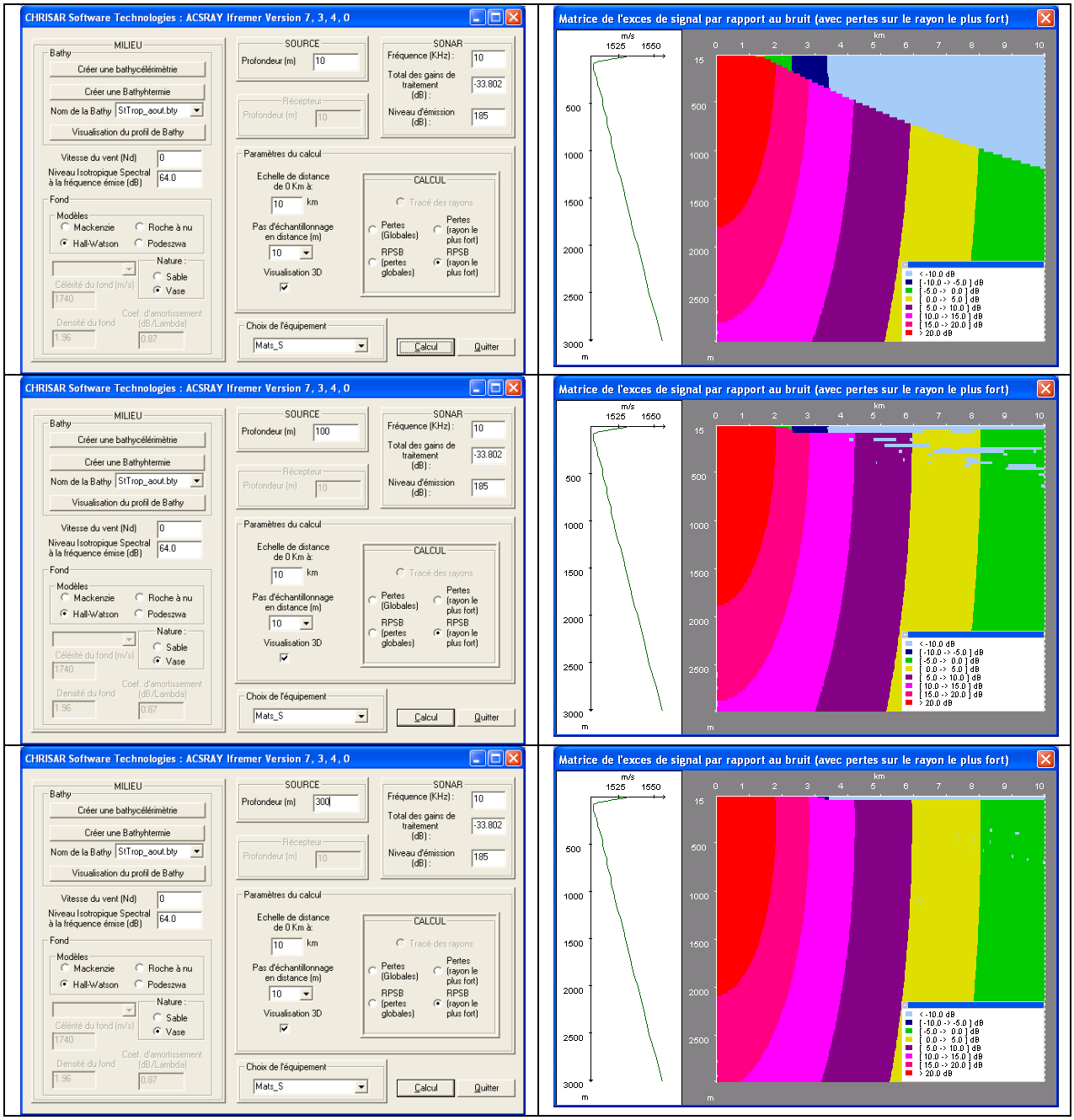

figure 5 a-c :propagation performances for sound velocity profiles in summer conditions

Mediterrenean Sea (Toulon - France) - Winter conditions

In winter periods, the water temperature is homogenous in the upper water layers, and sound velocity increases with pressure from the surface downwards. No shadow zones appear in the computation plots, and maximum range of about 3km is reached close to the surface. This maximum range slowly decreases with depth.

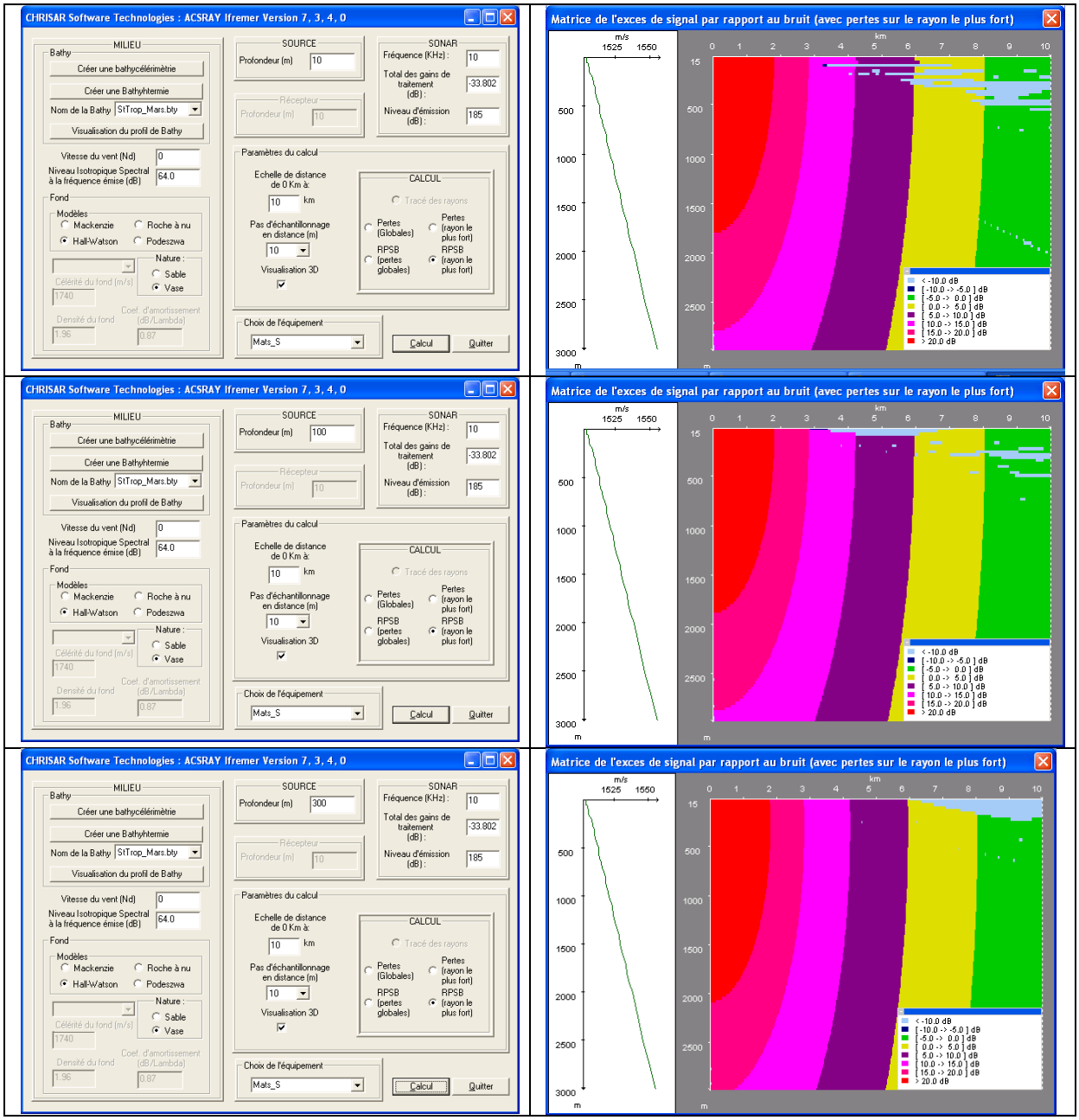

figure 7 a-c :propagation performances for sound velocity profiles in winter conditions

Estimation of range in function of receiver noise level

The acoustic and transmission parameters are the same as above.

In this case we vary the vehicle noise measured at the modem receiver by 10db steps. The technical and environmental parameters are those of the above paragraph in the more favorable winter conditions, both vehicles situated at 100m depth. The noise levels are fixed as 64dBµPa√Hz, 74dBµPa√Hz and 84dBµPa√Hz. 74dBµPa√Hz is a typical level experienced on IFREMER's AUVs. The maximum ranges will be 8km, 4.5km and 1.8km respectively.

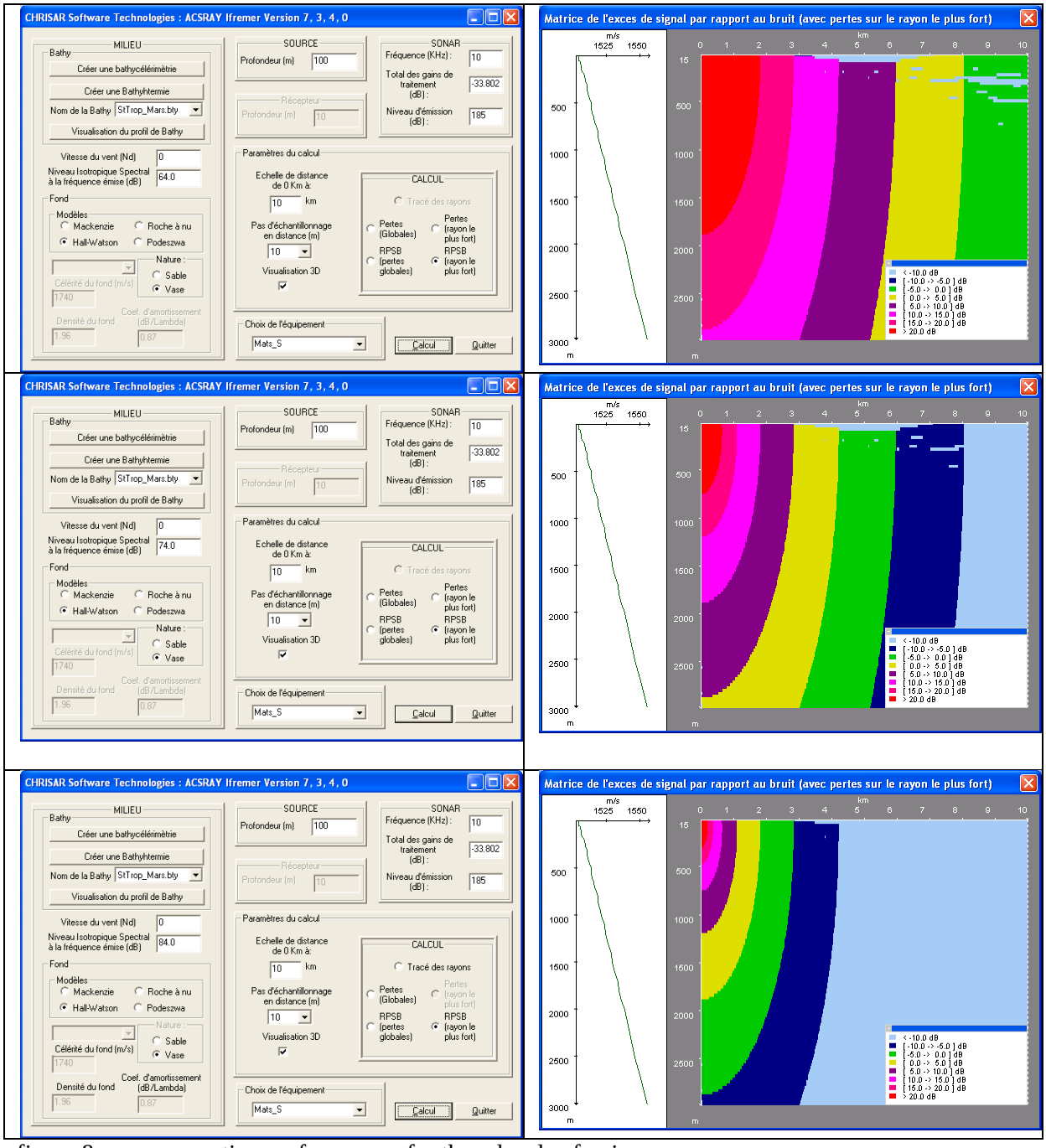

figure 8 a-c :propagation performances for three levels of noise

6. Complementary approaches

In the scientific research community specialized in underwater acoustic communications, significant achievements have been reached with novel digital signal processing approaches. The OFDM (Orthogonal Frequency Division Multiplexing) technique presented in the paragraph 8 of this document allows multi-channel communications (see also [3]). Another promising technique is MIMO (Multiple Input Multiple Output) array networks [4] – their potential lies in multiple channels between arrays of transmitters on one side and arrays of receivers on the other side.

The optimization results in a gain in the data rate performances. The necessary hardware (arrays) and the application constraints are not clear at the present stage of research.

7. Conclusions for AUV fleet control and simulation

Underwater vehicle simulator modules from previous work are being adapted to the FeedNetBack project work. Simulation functionalities cover three areas :

1. vehicle kinematic behavior and control of multiple vehicles;
2. communication between vehicles with a parametric model representing transmission delay, realistic data rates and risk of bad reception due to absorption, multi-path, ray bending etc.
3. environment model and geographically referenced sensor readings;

A complex simulation software suite with extensive 3D representations is being adapted from earlier work, partner INRIA (P01) is involved with development of a simplified simulator running on the *Matlab* ™ suite.

The acoustic communications network is implemented with performances according to D8.01 and D8.02 regarding range, bit-error and delay performances. The networking architecture implemented at the current stage is the TDMA concept (see D8.01 for details).

Complementary Bibilography

[1] M.Stojanovic, “Underwater Acoustic Communications: Design Considerations on the Physical Layer," in Proc. IEEE / IFIP Fifth Annual Conference on Wireless On demand Network Systems and Services (WONS 2008), Garmisch-Partenkirchen, Germany, January 2008.

[2] J.Preisig, “Acoustic propagation considerations for underwater acoustic communications network development,” in Proc. First ACM International Workshop on Underwater Networks (WuwNeT/Mobicom), Sept. 2006.

[3] M.Stojanovic, “OFDM for underwater acoustic communications: adaptive synchronization and sparse channel estimation,” submitted to ICASSP, 2008.

[4] J.-P. Bouvet, “Capacity analysis of underwater acoustic MIMO communications”, IEEE-Oceans 2010, Sidney, 24-27th May 2010

8. OFDM Receiver for underwater acoustic communications

This paragraph has been prepared by partner P01 INRIA. For reasons of different choice of text processing software, the styles are not identical with the first part of the document. Figure numbering is starting at 1 in this section. We hope to present a homogenous document in a second version.

Problem setting

Orthogonal Frequency Division Multiplexing (OFDM) has emerged as an attractive signaling scheme for modern wireless wideband communications such as 3GPP LTE, WIMAX, Wireless LANs, Digital TV Broadcasting (DVB), Vehicle to Vehicle (V2V) communications, and has recently been considered for underwater acoustic (UWA) communications. Interest in OFDM stems from the fact that it decomposes a time-invariant frequency selective channel into a set of independent sub-channels that are free of inter-symbol interference [1]. Since each subcarrier only experiences flat fading, complex time-domain equalizers are not necessary [2]. However, OFDM is highly sensitive to temporal channel variation, frequency offsets and motion-induced Doppler distortion, which destroy carrier orthogonality and introduce inter-carrier interference (ICI) . When ICI is not explicitly mitigated, the performance of conventional data detection schemes are severely degraded.

Underwater acoustic channels are typically wideband in nature due to the small ratio of carrier frequency to the signal bandwidth, which introduces frequency-dependent Doppler shifts [3]. They are particularly challenging since they encompass the behaviour of high-speed mobile radio-frequency channels and that of satellite communications (delay). The main characteristic of such channels are as follows:

- The available bandwidth is severely limited. The attenuation of acoustic signal increases with frequency and range [4]. Consequently, the feasible band is extremely small;
- The channel impulse response is not only spatially varied but also temporarily varied. The channel characteristics vary with time and highly depend on the location of the transmitter and receiver. The fluctuation nature of the channel causes the received signals to be easily distorted.
- The multi-path propagation of two types: macro-multipaths, which are the deterministic propagation paths; and micro-multipath, which is a random signal fluctuation. The macro-multipaths are caused by both reflection at the boundaries (bottom, surface and any object in the water) and bending. Intersymbol Interference (ISI) thus occurs. Compared with the spread of its ground-based counterpart, which is on the order of several symbol intervals, ISI spreading in an underwater acoustic channel is several tens or hundred of symbol intervals for moderate to high data rate in the horizontal channel. Micro-multipath fluctuations are mainly caused by surface wave, which contributes the most to the time variability of shallow water channel. [5];
- Propagation delay in underwater is five orders of magnitude higher than in radio frequency (RF) terrestrial channels, and extremely variable;
- High bit error rates and temporary losses of connectivity (shadow zones) can be experienced, due to the extreme characteristics of the underwater channel.

Recently, there have been extensive investigations on underwater OFDM communication. Some of them consider pilot-tone based block-by-block receiver. The block-by-block receiver does not rely on channel dependence across OFDM blocks, and thus it is robust to fast channel variations across OFDM blocks. In contrast to single carrier phase-coherent transmission, OFDM has one desirable property that one signal design can be easily scaled to fit into different transmission bandwidths with negligible changes on the receiver [6]. With bandwidth varying from 3 kHz to 50 kHz, data rates from 1.5 kbps to 25 kbps after rate 1/2 coding and QPSK modulation are reported in [6]. Further, with different bandwidths of 12 kHz, 25 kHz and 50 kHz, data rates of 12 kbps, 25 kbps, and 50 kbps after rate 1/2 coding and 16-QAM modulation are

also achieved [6]. These recent studies demonstrate the feasibility and flexibility of OFDM for underwater acoustic communication.

Multipath delay and Doppler effects constitute the main obstacles to robust underwater acoustic communication. One common approximation is to treat the channel as having a common Doppler scaling factor on all propagation paths. In order to adequately recover the transmitted information, algorithms at the receiver must include estimation and compensation of the Doppler scaling factor, channel estimation, and information symbols estimation.

For estimating the Doppler scaling factor, several approaches have been suggested in the literature (see [7] for example). In the OFDM case, they are based on the use of preamble and postamble of a packet consisting of multiple OFDM blocks [3] or by exploiting correlation induced by the cyclic prefix [8]. Then, the received signal is resampled by using a sampling period related to the estimated Doppler scaling factor. We derive new data detection schemes where Doppler estimation and channel estimation are solved by means of high resolution harmonic retrieval solvers [9, 10, 11]. In the proposed scheme, the received data are processed block-by-block. The advantage of the proposed scheme is to avoid data resampling and residual CFO estimation and compensation.

System model

We consider an OFDM transmission system where each OFDM block is constituted with two sub-blocks of respective length T_u and T_d, with $T_d/T_u \in \mathbb{N}$, as depicted in Fig. 1. Each sub-block is followed by a cyclic suffix (CS) of duration T_g. Therefore, the overall OFDM block duration is $T = T_u + T_d + 2T_g$.

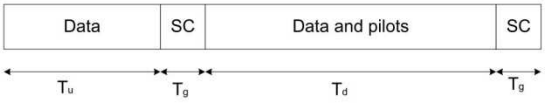

Figure 1: Structure of the OFDM block

We denote by c_q the data symbols in the first sub-block. They are all informative and thus unknown to the receiver. In the second sub-block, all data symbols d_k are not informative; some of them are known to the receiver and will serve to estimate the equivalent channel parameters. In baseband, the signal $s(.)$ to be transmitted can be viewed as a mixture of two signals $s_u(.)$ and $s_d(.)$, each one corresponding respectively to the first and to the second sub-blocks:

$$s(t) = s_u(t) + s_d(t) \tag{1}$$

with

$$\begin{aligned} s_u(t) &= \eta \sum_{q \in \mathcal{K}_u} c_q e^{j2\pi qQ\Delta f t} \Pi_{T_u+T_g}(t) \\ s_d(t) &= \sum_{k \in \mathcal{K}_d} d_k e^{j2\pi k\Delta f t} \Pi_{T_d+T_g}(t - T_u - T_g) \end{aligned}$$

where $\Delta f = 1/T_d$ denotes the minimal frequency spacing between consecutive subcarriers, Π_T allows taking the CS operation into account, i.e. $\Pi_T(t) = 1$, $t \in [0, T]$, and $\Pi_T(t) = 0$, otherwise, η allows controlling the power of the first sub-block so that both sub-blocks have the same power, Q is an integer that allows increasing the frequency spacing between the subcarriers in $s_u(.)$, $\mathcal{K}_u$ (resp. $\mathcal{K}_d$) the set of subcarriers in the first (resp. second) sub-block.

In the sequel, we consider that $\mathcal{K}_u \subset \mathcal{K}_d$, meaning that some of the subcarriers of the second sub-block are reused in the first sub-block. By denoting K_u (resp. K_d) the cardinality of $\mathcal{K}_u$ (resp. $\mathcal{K}_d$), i.e. the number of used subcarriers, we get $K_u < K_d$, $\mathcal{K}_d = \{-K_d/2, \cdots, K_d/2 + 1\}$, and $\mathcal{K}_u = \{q_0, \cdots, q_0 + K_u - 1\}$, for a given integer q_0.

In passband, the analytical representation of the signal to be transmitted is $x(t) = s_u(t)e^{j2\pi f_c t} + s_d(t)e^{j2\pi f_c t}$, $t \in [0, T]$, with f_c the central carrier frequency. This signal is transmitted through a multipath

underwater channel whose impulse response is given by:

$$h(t,\tau) = \sum_{p=1}^{P} A_p(t)\delta(\tau - \tau_p(t)),$$

where $A_p(t)$ and $\tau_p(t)$ are respectively the gain and the delay associated with the pth path. The following assumptions are adopted:

- All paths are affected by a similar Doppler scaling factor a such that $\tau_p(t) = \tau_p - at$.
- The path delays τ_p, the gains A_p, and the Doppler scaling factor a are constant over the block duration T.
- The guard interval T_g is chosen so that $T_g > \max\{\tau_p\} = \tau_{max}$.

Therefore, the received signal results on a mixture of scaled, dilated or compressed, and delayed versions of the original OFDM block as shown in Fig. 2. Hence, we can define two time windows I_1 and I_2 where

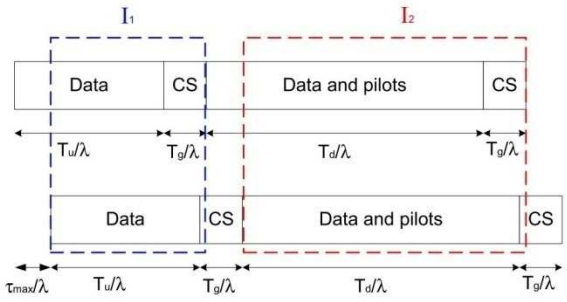

Figure 2: Multipath and Doppler effect on the OFDM block

the received signal strictly depends on the first and second sub-blocks respectively. These time windows are defined by: $I_1 = \left[\frac{\tau_{max}}{\lambda}, \frac{T_u+T_g+\tau_{min}}{\lambda}\right]$ and $I_2 = \left[\frac{T_u+T_g+\tau_{max}}{\lambda}, \frac{T+\tau_{min}}{\lambda}\right]$, where $\tau_{min} \leq \tau_p \leq \tau_{max}$, $p = 1, \cdots, P$, and $\lambda = 1 + a$.

In I_1 and I_2, the analytical representation of the received signal is respectively given as follows:

$$y(t) = \eta \sum_{q=q_0}^{K_u+q_0-1} B_q c_q e^{j2\pi(1+a)\varphi_q t} + w(t), \quad t \in I_1 \tag{2}$$

$$y(t) = \sum_{k=-K_d/2}^{K_d/2-1} B_k d_k e^{j2\pi(1+a)f_k t} + w(t), \quad t \in I_2 \tag{3}$$

where $\varphi_q = f_c + qQ\Delta f$, $f_k = f_c + k\Delta f$, $w(t)$ denoting the additive noise, $B_q = \sum_{p=1}^{P} A_p e^{-j2\pi\varphi_q\tau_p}$, and

$$B_k = \sum_{p=1}^{P} A_p e^{-j2\pi f_k\tau_p}. \tag{4}$$

In both I_1 and I_2, the received signal $y(.)$ can be respectively viewed as a mixture of K_u and K_d harmonics with constant magnitudes. In the sequel, we intend to solve the problem of Doppler scale factor estimation as a Harmonic retrieval one. We make use of these two time windows for first estimating the Doppler scaling factor and then recovering the informative symbols contained in the OFDM block. Since the time windows involved in the estimation process depend on λ, we assume that λ is bounded, such that $\lambda_{min} \leq \lambda \leq \lambda_{max}$. One can note that λ_{max} and λ_{min} are related to the maximal and minimal velocities

of the underwater vehicles, which can be *a priori* known. In addition, we assume that τ_{max} is known and $\tau_{min} = 0$. Therefore the involved time windows are modified as follows

$$I_1 = \left[\frac{\tau_{max}}{\lambda_{min}}, \frac{T_u + T_g}{\lambda_{max}}\right] \quad I_2 = \left[\frac{T_u + T_g + \tau_{max}}{\lambda_{min}}, \frac{T}{\lambda_{max}}\right]. \tag{5}$$

Owing to the CS, the time windows to be used are larger than those obtained when using a ZP scheme as in [10]. Obviously, with more observations, an improvement of the resulting estimation method is expected.

Doppler estimation

The harmonic retrieval problem has been extensively studied in the literature (see [12, 13, 14, 15] for example). In general the magnitude are assumed to be constant as in the case for $y(.)$ in I_1 and I_2. For solving (2) as a harmonic retrieval problem, we make use of the high resolution method called HTLS (*Hankel Total Least Squares*) [16]. This algorithm can be viewed as a special case of the ESPRIT algorithm [14] and also as a Total Least Squares variant of Kung et al.'s algorithm [17]. Resorting to a high resolution method is mandatory since the Doppler is to be estimated from a very slight deviation of the actual subcarrier frequencies. A search on discretized space of frequencies could need a very short step of discretization, implying a huge complexity. In other hand, FFT based methods have a lower bound of resolution incompatible in such a situation.

In the noiseless case, we consider the N samples y_n, $n = n_0, \cdots, N + n_0 - 1$, of the first portion (2) of the received signal:

$$y_n = \eta \sum_{q=q_0}^{K_u+q_0-1} c_q B_q e^{j2\pi\varphi_q(1+a)nT_e} = \eta \sum_{q=q_0}^{K_u+q_0-1} c_q B_q \phi_q^n, \tag{6}$$

T_s being the sampling period. In a harmonic retrieval problem, we aim to estimate both the poles $\phi_q = e^{j2\pi\varphi_q(1+a)T_s}$ and the magnitudes $\eta c_q B_q$ of the K_u harmonics.

For this purpose, let us first build with the samples y_n the following $L \times M$ Hankel matrix

$$\mathbf{Y} = \begin{pmatrix} y_{n_0} & y_{n_0+1} & y_{n_0+2} & \cdots & y_{n_0+M-1} \\ y_{n_0+1} & y_{n_0+2} & \iddots & \cdots & y_{n_0+M} \\ y_{n_0+2} & \iddots & \iddots & \cdots & y_{n_0+M+1} \\ \vdots & \iddots & \iddots & \vdots & \vdots \\ y_{n_0+L-1} & y_{n_0+L} & \cdots & \cdots & y_{n_0+N-1} \end{pmatrix},$$

with $N = L + M - 1$, $L > K_u$, $M \geq K_u$. It admits the Vandermonde decomposition:

$$\mathbf{Y} = \mathbf{S}_1 diag(\boldsymbol{\alpha}) \mathbf{T}_1^T, \tag{7}$$

where $\mathbf{S}_1$ and $\mathbf{T}_1$ are two Vandermonde matrices with ϕ_q as generators:

$$\mathbf{S}_1 = \begin{pmatrix} 1 & \cdots & 1 \\ \phi_{q_0} & \cdots & \phi_{K_u+q_0-1} \\ \vdots & \ddots & \vdots \\ \phi_{q_0}^{L-1} & \cdots & \phi_{K_u+q_0-1}^{L-1} \end{pmatrix} \in \mathbb{C}^{L \times K_u}$$

$$\mathbf{T}_1 = \begin{pmatrix} 1 & \cdots & 1 \\ \phi_{q_0} & \cdots & \phi_{K_u+q_0-1} \\ \vdots & \ddots & \vdots \\ \phi_{q_0}^{M-1} & \cdots & \phi_{K_u+q_0-1}^{M-1} \end{pmatrix} \in \mathbb{C}^{M \times K_u},$$

while $\boldsymbol{\alpha}$ contains the complex magnitudes of the K_u harmonics:

$$\boldsymbol{\alpha} = \eta \begin{pmatrix} c_{q_0} B_{q_0} \phi_{q_0}^{n_0} & \cdots & c_{K_u+q_0-1} B_{K_u+q_0-1} \phi_{K_u+q_0-1}^{n_0} \end{pmatrix}^T$$

We intend to estimate the Doppler scaling factor from the angle of the generators ϕ_q. In order to avoid any ambiguity since angles are obtained up to 2π, the sampling period can be selected such that the angle of the generators belongs to $[-\pi, \pi]$. For this purpose, it is enough to select T_s such that:

$$T_s \leq \frac{1}{2\lambda_{max} \max\{\varphi_q\}}. \tag{8}$$

It should be noted that this condition corresponds precisely to the Nyquist-Shannon sampling theorem condition applied to the Doppler scaled spectrum of the received signal. We can also derive the following proposition:

Proposition 1 *If the sampling period is such that $T_s \leq \frac{1}{2\lambda_{max} \max\{\varphi_q\}}$, the Vandermonde matrices $\mathbf{S}_1 \in \mathbb{C}^{L\times K_u}$ and $\mathbf{T}_1 \in \mathbb{C}^{M\times K_u}$, $L > K_u$, $M \geq K_u$, with $\phi_q = e^{j2\pi\varphi_q(1+a)T_s}$ as generators are full column rank.*

Proof 1 *The Vandermonde matrices loose their rank if at least two generators have the same angle modulo 2π. Owing to condition (8) on the sampling period we know that the angles of the generators belong to $[0, \pi]$. Therefore, the angle of the generator are all distinct modulo 2π. Thus, the resulting Vandermonde matrices are full column rank.*

Let us denote by $\hat{\phi}_q$ the poles estimated with the HTLS method (see [9] for details). If the sampling period T_s is chosen according to (8), then the angle of $\hat{\phi}_q$, denoted $\angle\hat{\phi}_q$, belongs to $[-\pi, \pi]$. We deduce the following estimator for the Doppler scaling factor:

$$\hat{a} = -1 + \frac{1}{K_u} \sum_{q=q_0}^{K_u+q_0-1} \frac{\angle\hat{\phi}_q}{2\pi\varphi_q T_e}. \tag{9}$$

One can note that such a Doppler scaling factor estimator is completely blind. However, since it is a SVD-based estimator, the computation load becomes significant when increasing K_u. So, we suggest to use few active subcarriers K_u. The choice of the optimal number is still an open question. Moreover, when dealing with subspace-based methods, the dimension of the initial matrix is very important. When applying HTLS, it has been shown that very good results are obtained for $L \times N - L + 1$ matrices where $L \in [N/3, 2N/3]$ [18].

Data detection

Now, for recovering the transmitted information symbols, we assume that some pilot symbols have been inserted in the second OFDM sub-block. We first estimates channel parameters using pilot symbols before recovering the informative symbols. Recall that the symbols c_q are informative whereas only some of d_k are also informative. The samples corresponding to the time interval I_2 are given by:

$$y_n = y(t)|_{t=nT_e} = \sum_{k=-K_d/2}^{K_d/2-1} d_k B_k e^{j2\pi(1+a)f_k n T_e}.$$

In matrix form, we get:

$$\mathbf{y} = \mathbf{H}\mathbf{b}, \tag{10}$$

with $\mathbf{y} = \begin{pmatrix} y_{n_1} & \cdots & y_{n_1+N_1-1} \end{pmatrix}^T$, $\mathbf{b} = \begin{pmatrix} b_{-K_d/2} & \cdots & b_{K_d/2-1} \end{pmatrix}^T$, $b_k = d_k B_k$, $\hat{\phi}_k = e^{j2\pi(1+\hat{a})f_k T_e}$, and

$$\mathbf{H} = \begin{pmatrix} \hat{\phi}_{-K_d/2}^{n_1} & \cdots & \hat{\phi}_{K_d/2-1}^{n_1} \\ \vdots & \ddots & \vdots \\ \hat{\phi}_{-K_d/2}^{n_1+N_1-1} & \cdots & \hat{\phi}_{K_d/2-1}^{n_1+N_1-1} \end{pmatrix} \in \mathbb{C}^{N_1\times K_d}.$$

It is straightforward to check that $\mathbf{H}$ is a full column rank matrix if $N_1 > K_d$ and $T_s \leq \frac{1}{2\lambda_{max} \max\{f_k\}}$. As a consequence, we can compute the least squares (LS) solution of (10) as:

$$\hat{\mathbf{b}} = \mathbf{H}^{\dagger}\mathbf{y} \tag{11}$$

where $\mathbf{H}^{\dagger}$ denotes the pseudo-inverse operator of the matrix $\mathbf{H}$. Since the entries of $\hat{\mathbf{b}}$ result on the product of a symbol d_k and the equivalent channel parameters B_k, without lack of generality, by assuming that the subcarriers numbered $k = 0, 1, \cdots, K_p - 1$, $K_p < K_d/2$, are devoted to pilot symbols, i.e. d_k,$k = 0, 1, \cdots, K_p - 1$, are known to the receiver, we get:

$$\hat{B}_k = \hat{b}_k / d_k. \tag{12}$$

Now, the question is: how constructing $\hat{B}_k$ associated with the information symbols from those estimated using the K_p pilots?

First, we can note that (4) can also be written as

$$B_k = \sum_{p=1}^{P} \gamma_p \zeta_p^k, \quad \gamma_p = A_p e^{-j2\pi f_c \tau_p}, \quad \zeta_p = e^{-j2\pi \Delta_f \tau_p}. \tag{13}$$

The expression above is particularly meaningful. Indeed, B_k can be viewed as a mixture of exponentials in the frequency domain. We can therefore obtain both γ_p and ζ_p by solving a harmonic retrieval problem.

Assuming that the number of significative paths P is known and provided $K_p \geq 2P$, we make use of the HTLS method for solving the problem (13) where B_k is replaced by its estimated value $\hat{B}_k$. For this purpose, we build an $L \times M$ Hankel matrix $\mathbf{B}$, with $K_p = L + M - 1$, $L > P$, $M \geq P$, which admits the following Vandermonde decomposition:

$$\mathbf{B} = \mathbf{S}_2 diag(\boldsymbol{\gamma}) \mathbf{T}_2^T. \tag{14}$$

with $\mathbf{S_2}$ and $\mathbf{T}_2$ some Vandermonde matrices having ζ_p as generators, and $\boldsymbol{\gamma}$ the vector with γ_p as entries. Let us denote $\hat{\zeta}_p$ the estimated poles. By replacing the poles by their estimated values in $\mathbf{S}_2$ and $\mathbf{T}_2$, we can solve the following equation:

$$vec(\mathbf{B}) = (\mathbf{T}_2 \odot \mathbf{S}_2)\, \boldsymbol{\gamma}, \tag{15}$$

$vec(.)$ denoting the vectorization operator whereas $\odot$ stands for the Khatri-Rao product, i.e. a columnwise Kronecker product.

The entries of the least squares solution of (15), denoted $\hat{\gamma}$, can be used for computing $\hat{B}_k$ for any value of k as $\hat{B}_k = \sum_{p=1}^{P} \hat{\gamma}_p \hat{\zeta}_p^k$. Therefore, we can deduce the information symbols in the second sub-block as:

$$\hat{d}_k = \frac{\hat{b}_k}{\sum_{p=1}^{P} \hat{\gamma}_p \hat{\zeta}_p^k}. \tag{16}$$

while those of the first sub-block can be obtained as

$$\hat{c}_q = \frac{\hat{\alpha}_q}{\eta e^{j2\pi\varphi_q(1+\hat{a})n_0 T_s} \sum_{p=1}^{P} \hat{\gamma}_p \hat{\zeta}_p^q}. \tag{17}$$

$\hat{\alpha}_q$ being the corresponding entry of the least squares solution of the vectorized version of equation (7), i.e. $vec(\mathbf{Y}) = (\mathbf{T}_1 \odot \mathbf{S}_1)\, \boldsymbol{\alpha}$.

Simulation results

In these simulations, the range of frequency used by the underwater vehicles was $[16kHz - 27kHz]$. The Doppler scaling factor was set to $a = 8 \times 10^{-4}$. We assume that $|a_{max}| = 10^{-3}$, meaning that the maximal relative speed is 1.5 m/s. The carrier frequency was set equal to $f_c = 21$ kHz, whereas the guard interval was $T_g = 10$ ms. We used $K_d = 256$ subcarriers for the second OFDM sub-block. The duration of this sub-block is $T_d = K_d/B$, with $B = 11$ kHz, whereas that of the first sub-block is $T_u = T_d/10$. Hence, the duration of one OFDM block is 45.6 ms. The data was modulated using a QPSK constellation. All the results presented below are averaged values over 100 independent Monte Carlo runs. The channel impulse response used for the simulation is depicted in figure 3. The additive noise was a complex valued white Gaussian noise.

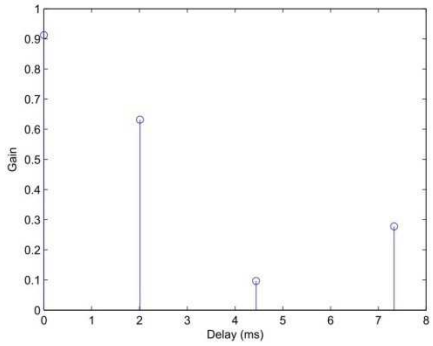

Figure 3: Impulse response of the simulated channel

We evaluate the performance of the proposed scheme by computing the mean square error between the estimated and the actual values of the Doppler scaling factor. The data detection method is evaluated by means of the bit-error-rate (BER).

Fig. 4 depicts the mean value of the estimated Doppler scaling factor whereas the mean square error on the estimation of this factor is depicted in Fig. 5.

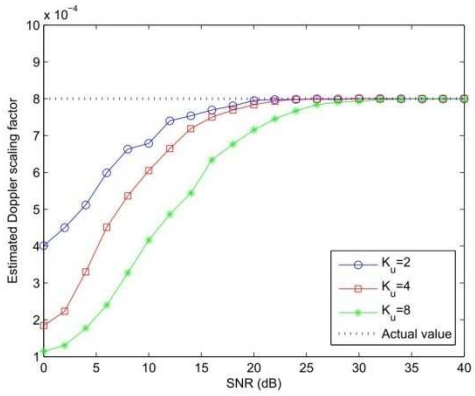

Figure 4: Estimated value of the Doppler scaling factor.

We can note the effectiveness of the Doppler estimation scheme. However, the performance is degraded when decreasing the SNR. The degradation is more accentuated when increasing the number of subcarriers in the first sub-block of the OFDM symbol. Indeed, by increasing K_u, the frequency spacing of the sub-carriers is reduced. Therefore, the harmonic retrieval problem needs higher resolution and precision. Such a precision is difficult to obtain when the SNR decreases. Increasing K_u seems to be relevant only for high SNR values. This observation is directly related to the behaviour of HTLS in noisy cases.

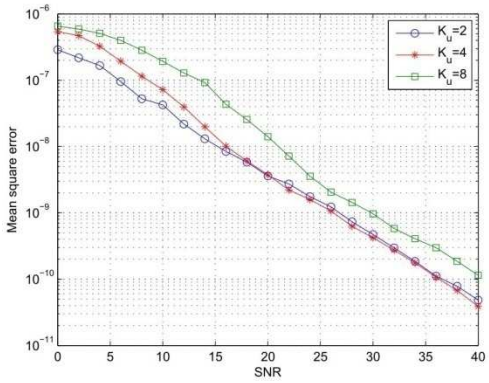

Figure 5: Mean Square Error for the estimation of the Doppler scaling factor.

In Fig. 6, we depict the BER for three numbers K_p of pilots and two values for K_u. Increasing the number of pilot allows improving the BER.

From these simulations, we can conclude that increasing the number of pilots has a positive effect on the performance of the receiver while increasing the number of subcarriers K_u has a contrary effect.

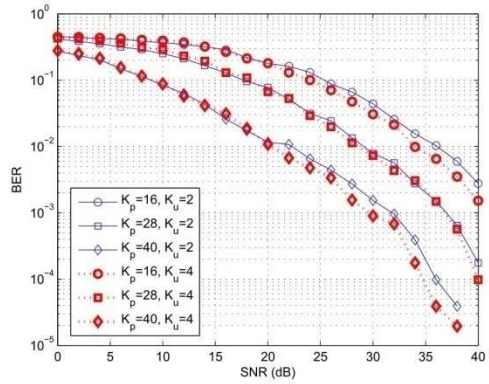

Figure 6: BER for different number of pilots and two numbers of subcarriers in the first sub-block ($K_d = 256$)

Multiple access channel methods

In a network of multiple AUVs, multiple access techniques constitute a crucial question.

Frequency Division Multiple Access (FDMA) divides the available bandwidth into several sub-bands and assigns one of them to a particular user. The band is used by this user only till it is released. FDMA has been deployed successfully in ground-based radio networks. However, FDMA may not be a good fit in underwater environment. The available bandwidth is extremely limited for acoustic signal underwater. If we divide the band into several even smaller parts, the coherence bandwidth of the transmission channel can be bigger than an FDMA sub-channel. Correspondingly, fading is caused among users with different sub-bands [19].

Time Division Multiple Access (TDMA) is another basic access technology. In this technology, a time frame is divided into multiple time slots and a slot is assigned to one individual user. Each user transmits in the assigned slot. TDMA has been widely deployed for ground-based radio networks and several 2G cellular network standards (GSM , IS 136) are based on the idea of TDMA. It is also used extensively in satellite communication systems. One advantage of TDMA is energy saving, which is extremely important

in underwater environment. Since each user only transmits on its assigned slot and keeps idle in other time slots, the transmitter could be turned off during aforementioned idle period, such that energy can be saved. Another advantage is its flexibility. The same hardware can be used to transmit and no extra hardware is needed for other operations, e.g., to add another time slot for a user. One of the disadvantages is its overhead. To avoid collision from neighboring slots, guard times that are proportional to the propagation time delay is included. The overhead is found larger than that of FDMA [20]. Another drawback is that it is hard to achieve time synchronization, which is a necessity for TDMA technology, in an underwater environment, due to the more significant difference in propagation delays. Consequently, collisions happen and the system throughput decreases.

Code Division Multiple Access (CDMA), which is based on spread spectrum techniques, is another widely deployed access method. In contrast with FDMA and TDMA, CDMA does not divide time or frequency. It allows users to transmit all the time with all the available bandwidth. Users are distinguished by allocating to each user a spreading code. This code is orthogonal with any other spreading codes that other users take. CDMA technology has been used widely for ground-based wireless networks, especially for cellular networks and military networks. It is one of the popular standards of 2G cellular networks (IS-95), 3G systems (CDMA 2000 and UMTS) and in 4G systems when combined with OFDM technology. However, a multi-user CDMA system needs good power control strategy to work properly. Otherwise, the near-far problem could deteriorate its performance [20]. Power control is easily implemented in ground-based radio networks, but it is hard to do so in underwater environment.

Orthogonal Frequency Division Multiple Access (OFDMA) is one of the recently proposed multiple access methods. It is the main choice for future broadband communication networks, e.g., WiMAX, LTE (Long Term Evolution), and IEEE 802.11n. The proposed data detection scheme derived in the previous sections can be used in a TDMA framework and can be extended to the OFDMA case. In the OFDMA case, one can significantly reduce the latency induced by the TDMA scheme. In OFDMA, a subset of orthogonal sub-carriers are allocated to each user. If the subsets are adequately chosen, the bandwidth used by each user can be larger than that allowed by the FDMA scheme as depicted in Fig. 7. Indeed, by allocating consecutive subcarriers to different users, the frequency spacing between subcarriers associated with a given user increases. And the bandwidth is larger than in a scheme where consecutive subcarriers are allocate to the same users.

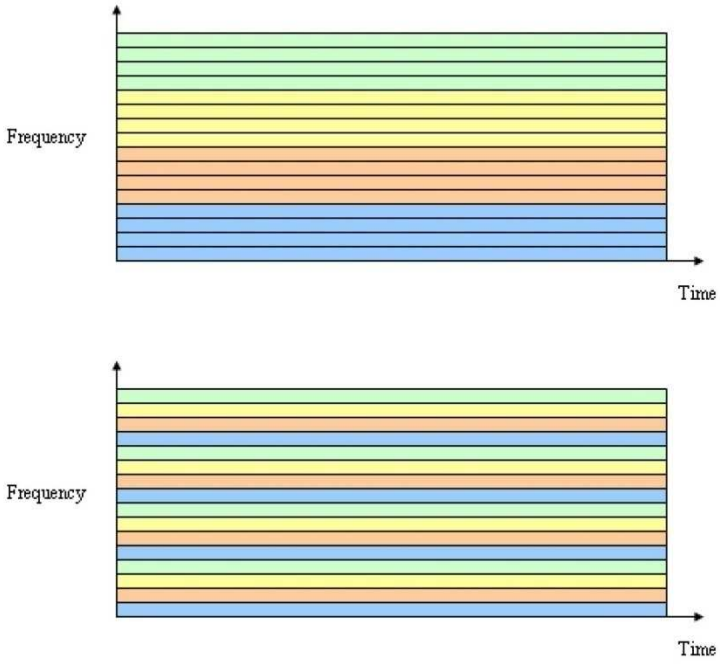

Figure 7: Frequency allocation in FDMA (Top) and OFDMA (Bottom).

Conclusion

We have presented a new scheme for both estimating the Doppler scaling factor and detecting the informative data. In the proposed scheme, each OFDM symbol is divided in two parts. The first one is shorter and carries out few data with few subcarriers whereas the second one contains both informative and pilot symbols. The first sub-block serves to estimate the Doppler scaling factor while the pilots in the second sub-block are used for estimating the equivalent channel. Both estimation methods are based on high resolution methods for solving harmonic retrieval problems in time and frequency domains respectively. The proposed scheme is particularly efficient for moderate to high SNR. Robustness to noise, for lower levels of SNR, and extension to the multi-user case will be investigated. In addition, effectiveness of the proposed approach using experimental data is to be considered in future works.

References

[1] S. Yerramalli, M. Stojanovic, and U. Mitra, "Partially FFT demodulation: a detection method for Doppler distorted OFDM systems," in *Proc. of 11th IEEE Int. IEEE International Workshop on Signal Processing Advances in Wireless Communications (SPAWC)*, Marrakesh, Morocco, 2010.

[2] A. Bahai and B. Saltzberg, *Multi-carrier digital communications: theory and applications of OFDM*. Springer, 1999.

[3] B. Li, S. Zhou, M. Stojanovic, L. Freitag, and P. Willett, "Multicarrier communication over underwater acoustic channels with nonuniform doppler shifts," *IEEE Journal of Oceanic Engineering*, vol. 33, no. 2, pp. 198–209, 2008.

[4] M. Stojanovic, "On the relationship between capacity and distance in an underwater acoustic communication channel," *ACM Sigmobile mobile Computing and Communications Review*, vol. 11, pp. 34–43, October 2007.

[5] R. Galvin and R. Coates, "Analysis of the performance of an underwater acoustic communications system and comparison with a stochastic model," in *Proc. OCEANS '94. 'Oceans Engineering for Today's Technology and Tomorrow's Preservation.'*, vol. 3, September 1994, pp. III/478–III/482.

[6] B. Li, S. Zhou, J. Huang, and P. Willett, "Scalable OFDM design for underwater acoustic communications," in *Proc. of ICASSP'08*, Las Vegas, NV, USA, 2008.

[7] B. Sharif, J. Neasham, O. Hinton, and A. Adams, "A computationally efficient doppler compensation for underwater acoustic communications," *IEEE Journal of oceanic engineering*, vol. 25, no. 1, pp. 52–61, January 2000.

[8] B.-C. Kim and I.-T. Lu, "Parameter study of OFDM underwater communications system," in *Proc. of OCEANS 2000 MTS/IEEE Conference and Exhibition*, vol. 2, September 11-14 2000, pp. 1251–1255.

[9] A. Kibangou, C. Siclet, and L. Ros, "Joint channel and doppler estimation for multicarrier underwater communications," in *Proc. of IEEE Int. Conf. on Acoustics, Speech, and Signal Processing (ICASSP) 2010*, Dallas, Tx, USA, March 14-19 2010.

[10] ——, "Zf ofdm receiver for underwater communications," in *Proc. of Int. Symp. on Communications, Control and Signal Processing (ISCCSP) 2010*, Limassol, Cyprus, March 3-5 2010.

[11] A. Kibangou, L. Ros, and C. Siclet, "Doppler estimation and data detection for underwater acoustic ZF-OFDM receiver," in *Proc. of the 7th IEEE Int. Symposium on Wireless Communication Systems (ISWCS)*, York, UK, September 19-22 2010.

[12] S. Kay, *Modern spectral estimation, Theory and Application*. Englewood Cliffs, New Jersey, USA: Prentice-Hall, 1988.

[13] P. Stoica and R. Moses, *Introduction to spectral analysis*. Englewood Cliffs, New Jersey, USA: Prentice-Hall, 1997.

[14] R. Roy and T. Kailath, "ESPRIT-Estimation of signal parameters via rotational invariance techniques," *IEEE Trans. on Signal Proc.*, vol. 37, no. 7, pp. 984–995, July 1989.

[15] J. Papy, L. De Lathauwer, and S. Van Huffel, "Exponential data fitting using multilinear algebra: The single-channel and multi-channel case," *Numer. Linear Algebra Appl.*, vol. 12, pp. 809–826, 2005.

[16] S. Van Huffel, "Enhanced resolution based on minimum variance estimation and exponential data modeling," *Signal Processing*, vol. 33, no. 3, pp. 333–355, 1993.

[17] S. Kung, K. Arun, and D. Bhaskar Rao, "State-space and singular value decomposition-based approximation methods for harmonic retrieval problem," *Journal of the Optical Society of America*, vol. 73, no. 12, pp. 1799–1811, 1983.

[18] S. Van Huffel, H. Chen, C. Decanniere, and P. Van Hecke, "Algorithm for time-domain NMR data fitting based on total least squares," *Journal of Magnetic Resonance*, vol. 110, no. series A, pp. 228–237, 1994.

[19] E. Sozer, M. Stojanovic, and J. Proakis, "Underwater acoustic networks," *IEEE Journal of Oceanic Engineering*, vol. 25, no. 1, pp. 72–83, January 2000.

[20] T. Rappaport, *Wireless communications*. Englewood Cliffs,NJ: Prentice Hall,, 1996.